The 12th Symposium on Polar Science
15 – 18 November 2021

National Institute of Polar Research
Research Organization of Information and Systems

Session OS
Space and upper atmosphere sciences

Program and Abstracts

Convener: Yoshimasa Tanaka (NIPR)

【OS】Space and upper atmospheric sciences

Scopes

This session covers the solar-terrestrial science related to topics in the polar upper atmosphere, ionosphere and magnetosphere.

Conveners : **Yoshimasa Tanaka (NIPR)**

Real-time Oral presentations (11:00 – 12:00, 13:30 - 17:30)

Date: Wed. 17 November

Chair: Takanori Nishiyama (NIPR)				
OSo1	11:00-11:15	Study of atmospheric instabilities in the polar upper mesosphere between 80 and 105 km above Tromsoe	*Satonori Nozawa(Nagoya University)	OSo1_Nozawa_00606_01.pdf
OSo2	11:15-11:30	Response of the semidiurnal tide in the polar lower thermosphere to variations in solar activity	*Hirotaka Koyama(Nagoya University), Satonori Nozawa(Institute for Space-Earth Environmental Research, Nagoya University), Yasunobu Ogawa(National Institute of Polar Research), Asgeir Brekke(UiT The Arctic University of Norway)	OSo2_Koyama_00120_01.pdf
OSo3	11:30-11:45	Night sky condition over Syowa Station deduced from all-sky images by a color digital camera	*Satoshi Ishii(Meiji University), Hidehiko Suzuki(Meiji University), Akira Kadokura(NIPR), Mitsumu Ejiri(NIPR)	OSo3_Ishii_00529_01.pdf
OSo4	11:45-12:00	Mesospheric ionization impact of energetic electron precipitation during substorm growth phase	*Kiyoka Murase(SOKENDAI), Ryuho Kataoka(NIPR), Takanori Nishiyama(NIPR), Koji Nishimura(Kyoto University), Taishi Hashimoto(NIPR), Yoshimasa Tanaka(NIPR), Akira kadokura(NIPR), Yoshihiro Tomikawa(NIPR), Masaki Tsutsumi(NIPR), Yasunobu Ogawa(NIPR), Herbert Akihito Uchida(ISAS/JAXA), Kaoru Sato(University of Tokyo), Satoshi Kasahara(University of Tokyo), Takefumi Mitani(ISAS/JAXA), Shoichiro Yokota(Osaka University), Tomoaki Hori(Nagoya University), Kunihiro Keika(University of Tokyo), Takeshi Takashima(ISAS/JAXA), Yoshiya Kasahara(Kanazawa University), Shoya Matsuda(ISAS/JAXA), Masafumi Shoji(Nagoya University), Ayako Matsuoka(Kyoto Univ.), Iku Shinohara(ISAS/JAXA), Yoshizumi Miyoshi(Nagoya Univ.), Tatsuhiko Sato(JAEA), Yusuke Ebihara(Kyoto Univ.), Takashi Tanaka(Kyushu Univ.)	OSo4_Murase_00472_01.pdf

Lunch

Chair: Yoshimasa Tanaka (NIPR)				
OSo5	13:30-14:00	[I] Modeling of SEP-induced auroral emission: Global diffuse aurora on Mars and polar-glow aurora on Earth	*Yuki Nakamura(Tohoku University, Sorbonne Universite), Naoki Terada(Tohoku University), Francois Leblanc(Sorbonne Universite), Ali Rahmati(University of California), Ryuho Kataoka(NIPR, SOKENDAI), Kiyoka Murase(NIPR, SOKENDAI), Hiromu Nakagawa(Tohoku University), Shotaro Sakai(Tohoku University), Sayano Hiruba(Tohoku University)	OSo5_Nakamura_00541_01.pdf

OSo6	14:00-14:15	AuroraX project for space weather and space climate research in Antarctica	*Ryuho Kataoka(NIPR)	OSo6_Kataoka_00210_01.pdf
OSo7	14:15-14:30	Formation of Polar Cap Plasma Hole	*Takahiro Obara(PPARC. Tohoku University)	OSo7_Obara_00508_01.pdf
OSo8	14:30-14:45	SENSU SuperDARN JARE phase X and future direction	*Akira Sessai Yukimatu(NIPR, SOKENDAI), Nozomu Nishitani(ISEE, Nagoya Univ.), Tsutomu Nagatsuma(NICT), Tomoaki Hori(ISEE, Nagoya Univ.), Keisuke Hosokawa(Univ. of Electro-Communications), Masakazu Watanabe(ICSWSE, Kyushu Univ.), Hideaki Kawano(ICSWSE, Kyushu Univ.), Yusuke Ebihara(RISH, Kyoto Univ.), Hideo Maeno(NICT), Ryuho Kataoka(NIPR, SOKENDAI), Yoshimasa Tanaka(ROIS-DS PEDSC, NIPR, SOKENDAI), Koji Nishimura(RISH, Kyoto Univ.), Natsuo Sato(NIPR), Yuka Kadowaki(ROIS-DS PEDSC)	OSo8_Yukimatu_00F19:F22df
Chair: Akira Sessai Yukimatu (NIPR)				
OSo9	14:45-15:00	Analysis of the Summer Solstice Storm 2015 based on the “reanalysis data” of the space weather	*Shigeru Fujita(ROIS-DS, ISM), Takanori Nishiyama(NIPR), Akira Kadokura(ROIS-DS, NIPR), Yoshimasa Tanaka(ROIS-DS, NIPR)	OSo9_Fujita_00559_01.pdf
OSo10	15:00-15:15	Modular Design for the Reproduce Plasma Universe (REPPU) code	*Satoko Saita(National Institute of Technology, Kitakyushu College), Shigeru Fujita(ROIS-DS, ISM), Takashi Tanaka(ICSWSE, Kyushu University)	OSo10_Saita_00211_01.pdf
OSo11	15:15-15:30	Correction of atmospheric effect on Cosmic Ray count rate by machine learning	*Shunta Asano(Shinshu University)	OSo11_Asano_00610_01.pdf
OSo12	15:30-15:45	Magnetospheric-density estimation from SuperDARN VLOS data to identify magnetospheric regions, by identifying FLR events in ionospheric or ground/sea backscatters	*Hideaki Kawano(Kyushu University), Akira Sessai Yukimatu(National Institute of Polar Research, and Department of Polar Science, SOKENDAI, Japan), Nozomu Nishitani(Institute for Space-Earth Environmental Research, Nagoya University, Japan), Yoshimasa Tanaka(National Institute of Polar Research, and Department of Polar Science, SOKENDAI, Japan), Satoko Saita(National Institute of Technology, Kitakyushu College, Japan), Tomoaki Hori(Institute for Space-Earth Environmental Research, Nagoya University, Japan)	OSo12_Kawano_00168_01.pdf
	15:45-16:00	break		
Chair: Kataoka Ryuho (NIPR)				
OSo13	16:00-16:30	[I] Preparations and objectives for the 4 December 2021 solar eclipse over Antarctica	*Mervyn Paul Freeman(British Antarctic Survey), Michael Hartinger(Space Sciences Institute), Xueling Shi(Virginia Polytechnic Institute and State University), James Weygand(Institute of Geophysics and Planetary Physics, University of California, Los Angeles)	OSo13_Freeman_00555_01.pdf

OSo14	16:30-17:00	[I] Optical and radar observations of neutral heating by auroral electrodynamics	*Daniel Whiter(University of Southampton), David Price(University of Southampton, UK)	OSo14_Whiter_00622_01.pdf
OSo15	17:00-17:15	Effects of CIR- and CME-driven magnetic storm on ion upflows in the low-altitude ionosphere	*Masayoshi Takada(The University of Tokyo), Kanako Seki(The University of Tokyo), Yasunobu Ogawa(National Institute of Polar Research, Japan)	OSo15_Takada_00231_01.pdf
OSo16	17:15-17:30	Antarctic large area network observation of auroral phenomena using unmanned system: Current status of project in 2021	*Akira Kadokura(ROIS-DS,PEDSC)	OSo16_Kadokura_00616_01.pdf

Real-time Oral presentations (9:00 – 11:45)

Date: Thu. 18 November

Chair: Yoshimasa Tanaka (NIPR)				
OSo17	9:00-9:15	Role of the FAC in transmitting substorm disturbances in the M-I coupling system	*Takashi Tanaka(Kyushu University)	OSo17_Tanaka_00504_01.pdf
OSo18	9:15-9:30	A possible origin of the “polar cap bifurcation” during northward interplanetary magnetic field periods	*Masakazu Watanabe(Kyushu University), Dongsheng Cai(University of Tsukuba), Peikun Xiong(University of Tsukuba), Shigeru Fujita(The Institute of Statistical Mathematics), Takashi Tanaka(Kyushu University)	OSo18_Watanabe_00216_01.pdf
OSo19	9:30-9:45	Dependence of magnetospheric plasma density profile on solar and magnetic activity in the Japanese meridian plane	*Aoi Onaka(Kyushu University), Hideaki Kawano(1.Department of Earth and Planetary Sciences, Faculty of Science, Kyushu University 2.International Center for Space Weather Science and Education, Kyushu University), Teiji Uozumi(International Center for Space Weather Science and Education, Kyushu University), Shuji Abe(International Center for Space Weather Science and Education, Kyushu University), Akimasa Yoshikawa(1.Department of Earth and Planetary Sciences, Faculty of Science, Kyushu University 2.International Center for Space Weather Science and Education, Kyushu University)	OSo19_Onaka_00552_01.pdf
OSo20	9:45-10:00	Identification of Field Line Resonances using Machine Learning Algorithms	*Satoko Saita(National Institute of Technology, Kitakyushu College), Akiko Fujimoto(Kyushu Institute of Technology Research Center for Data Science), Yuki Obana(Department of Engineering Science, Osaka Electro-Communication University)	OSo20_Saita_00211_02.pdf
OSo21	10:00-10:15	Plan and progress report on the imaging receiver system at the SuperDARN Hokkaido East radar	*Nozomu Nishitani(Nagoya University)	OSo21_Nishitani_00193_01.pdf
	10:15-10:30	break		
Chair: Akira Kadokura (NIPR)				

OSo22	10:30-10:45	Characteristics of wave in the plasmasphere during global-mode wave events: Analysis of data from ground magnetometers at middle and low latitudes	*Yuta Yamatani(Kyushu University), Hideaki Kawano(1.International Center for Space Weather Science and Education, Kyushu University 2.Department of Earth and Planetary Sciences, Faculty of Science, Kyushu University), Akimasa Yoshikawa(1.International Center for Space Weather Science and Education, Kyushu University 2.Department of Earth and Planetary Sciences, Faculty of Science, Kyushu University)	OSo22_Yamatani_00551_01.pdf
OSo23	10:45-11:00	Atmospheric Electric Field Variations during Auroral Substorm Events	*Yasuhiro Minamoto(Mount Fuji Research Station), Masashi Kamogawa(University of Shizuoka), Akira Kadokura(National Institute of Polar Research), Yoshimasa Tanaka(National Institute of Polar Research), Mitsuteru Sato(Graduate School of Science, Hokkaido University)	OSo23_Minamoto_00560_01.pdf
OSo24	11:00-11:15	Precipitating electron energy of pulsating aurora estimated from all-sky multi-wavelength observations	*Kohei Toyama(Nagoya University), Satoshi Kurita(Kyoto University), Yoshizumi Miyoshi(Nagoya University, ISEE), Keisuke Hosokawa(The University of Electro-Communications), Shinji Saito(NICT), Yasunobu Ogawa(National Institute of Polar Research), Shin-ichiro Oyama(Nagoya University, ISEE), Tetsuya Kawabata(Nagoya University, ISEE), Kazushi Asamura(Institute of Space and Astronautical Science)	OS24_Toyama_00607_01.pdf
OSo25	11:15-11:30	Auroral tomography analysis considering auroral type	*Yoshimasa Tanaka(PEDSC, ROIS-DS), Yasunobu Ogawa(National Institute of Polar Research), Mizuki Fukizawa(Tohoku University), Takeshi Sakanoi(Tohoku University), Keisuke Hosokawa(The University of Electro-Communications), Takuo Tsuda(The University of Electro-Communications), Akira Kadokura(National Institute of Polar Research)	OSo25_Tanaka_00222_01.pdf
OSo26	11:30-11:45	Yearly variations in Be-7 concentrations in the surface air at Iceland and Japan for 17 years from 2003: Solar modulation of cosmogenic nuclide	*Hirohisa Sakurai(Yamagata University), Youmei Kawamura(Faculty of Science, Yamagata University), Fuyuki Tokanai(Faculty of Science, Yamagata University), Emiko Inui(Yamagata University), Mirei Takeyama(Faculty of Science, Yamagata University), Toru Moriya(Faculty of Science, Yamagata University), Fusa Miyake(ISEE, Nagoya University), Akira Kadokura(NIPR), Natsuo Sato(NIPR), Bj*rnsson Gunnlaugur(Science Institute, Iceland University)	OSo26_Sakurai_00099_01.pdf

Study of atmospheric instabilities in the polar upper mesosphere between 80 and 105 km above Tromsø

Satonori Nozawa[1], Takuya Kawahara[2], Norihito Saito[3], Satoshi Wada[3], Takuo T. Tsuda[4], and Tetsuya Kawabata[1]
[1]*Institute for Space-Earth Environmental Research, Nagoya University*
[2]*Faculty of Engineering, Shinshu University*
[3]*RIKEN Center for Advanced Photonics, RIKEN*
[4]*Department of Communication Engineering and Informatics, The University of Electro-Communications*

We have studied the atmospheric stability between 80 and 105 km above Tromsø (69.6ºN, 19.2ºE) using temperature and wind data obtained by the sodium LIDAR at Tromsø (69.6ºN, 19.2ºE) (Nozawa et al., 2014). First, we have calculated Brunt-Väisälä frequency (N) for 365 nights from October 2010 to December 2019, and Richardson number (Ri) for 265 nights between October 2012 to December 2019. Second, using those values (N and Ri), we have calculated probabilities of the static instability (N<0) and the dynamic instability (0=<Ri<0.25) that can be used for proxies for evaluating the atmospheric instability (Zhao et al., 2003). When we use data with 6 min/1 km resolutions, the probability of the static instability varies from about 3% to 27% with a mean value of 12%, while that of the dynamic instability varies from 7% to 31% with a mean value of 15%. Both the probabilities show no clear monthly/seasonal variations from October to March.

The probability of the static instability does not show clear solar cycle dependence (F10.7 index), while it shows a slight dependence of geomagnetic activity (K-index) (its correlation coefficient being 0.27). The probability of the static instability between 95 and 100 km shows higher dependence of geomagnetic activity (K-index) (its correlation coefficient being 0.47). This would suggest an auroral effect would influence on the atmospheric stability in the polar upper mesosphere. On the other hand, the probability of the dynamic instability shows solar cycle dependence (its correlation coefficient being 0.50), while it does not show dependence of geomagnetic activity. Furthermore, we have derived 12 h periodic components (assuming the semidiurnal tide) for 119 nights, and have compared them with the probabilities to evaluate possible contributions of the 12 h wave to the stabilities. The probability of the dynamic instability shows dependence of the 12hr wave amplitude (meridional and zonal wind component) (its correlation coefficient being 0.56 and 0.47, respectively), but that of the static instability has no dependence of it.

Acknowledgements
We thank TGO, UiT The Arctic University of Norway for providing the K-index data.

References

Nozawa, S., T. D. Kawahara, N. Saito, C. M. Hall, T. T. Tsuda, T. Kawabata, S. Wada, A. Brekke, T. Takahashi, H. Fujiwara, Y. Ogawa, and R. Fujii, Variations of the neutral temperature and sodium density between 80 and 107 km above Tromsoe during the winter of 2010-2011 by a new solid state sodium LIDAR, *J. Geophys. Res., 119*, doi:10.1002/2013JA019520, 441-451, 2014.

Zhao, Y., A. Z. Liu, and C. S. Gardner, Measurements of atmospheric stability in the mesopause region at Starfire Optical Range, NM, *J. Terr. Sol. Atmos. Phys., 65*, 219-232, 2003.

Response of the semidiurnal tide in the polar lower thermosphere to variations in solar activity

Hirotaka Koyama[1], Satonori Nozawa[1], Yasunobu Ogawa[2], Asgeir Brekke[3]
[1]*Institute for Space-Earth Environmental Research, Nagoya University, Nagoya, Aichi, Japan*
[2]*National Institute of Polar Research, Tachikawa, Tokyo, Japan*
[3]*UiT The Arctic University of Norway, Tromsø, Norway*

We will report solar activity dependence of the semidiurnal tide in the polar lower thermosphere.

Pancheva et al. (2003) showed that ozone amount increases with increasing solar activity from January 1989 to May 1993 using Total Ozone Mapping Spectrometer (TOMS) data near Sheffield in the UK (53° N; 4° W). This may be due to the shift of photochemical reactions towards ozone production when solar activity is high. They also showed that a positive linear relationship exists between the variance of total ozone, the variance of the semidiurnal tidal amplitudes (observed by meteor radar with no height finding) and the F10.7 solar activity proxy. On the other hand, Liu and Richmond (2013) pointed out the molecular viscosity decreases with lower solar activity, and the waves originating from the lower atmosphere generally become stronger under solar minimum conditions.

Nozawa and Brekke (1999a, b) investigated the solar activity dependence of the semidiurnal tide in the polar lower thermosphere during quiet geomagnetic activity. They reported that the semidiurnal tidal amplitude in summer does not show solar activity dependence, while in winter and equinox it shows solar activity dependence. The insufficient number of data, however, prevented them from distinguishing solar activity, geomagnetic activity, and seasonal dependence. In this study, we have gathered 328 day data, and then classify not only the solar activity, but also season and geomagnetic activity, and investigate the variation of the semidiurnal tide under each condition. In order to study the influence from the lower atmosphere, we classify the stratospheric ozone amount and evaluate how the ozone amount affects the semidiurnal tide.

In this study, neutral wind velocity data derived from ion velocity data at altitudes of 93-119 km for 33 years (1986-2019) obtained by the EISCAT UHF radar are used. Solar activity F10.7 is classified into three categories; low (F10.7≤75), middle (75<F10.7<150), and high (150≤F10.7). Neutral wind velocities under each condition are averaged at each time and altitude (6 minutes and 3-4 km, respectively). The 12-hour components are extracted using the Lomb-Scargle method (Lomb, 1976; Scargle, 1982). The 12-hour component is treated as semidiurnal tide. The local time of maximum (LTM) is also derived by the least-squares fitting.

We have found solar activity dependence of the semidiurnal tide in the polar lower thermosphere;
(1) Regardless of the season and geomagnetic activity, the amplitude increases with increasing solar activity; the amplitude increases by 30 m/s from low solar activity (F10.7≤75) to high solar activity (150≤F10.7) in summer.
(2) Solar activity dependence is stronger in summer than in winter. The difference of amplitude increment from low to high solar activities between summer and winter is about 10 m/s.

As mentioned above, we focus on ozone amount which plays an important role in generation of the semidiurnal tide. We discuss a correlation between ozone amount and solar activity (F10.7), and influence of ozone amount on the semidiurnal tide in the polar lower thermosphere for the period 1987-2018 using TOMS and Aura Ozone Monitoring Instrument (OMI). Since ozone data are not available in winter in the polar region, we use 242 day data in summer close to Tromsø. Derived correlation coefficient between ozone amount near Tromsø and solar activity (F10.7) during 1987-2018 is 0.18; suggesting the ozone amount has no solar activity dependence.

Acknowledgements

Earth Probe TOMS and Aura OMI daily total ozone data were provided by NASA Goddard Space Flight Center, USA, from their website at https://ozonewatch.gsfc.nasa.gov/

References

Liu, H.-L., and A. D. Richmond, Attribution of ionospheric vertical plasma drift perturbations to large-scale waves and the dependence on solar activity, *J. Geophys. Res. Space Physics*, **118**, 2452–2465, 2013.

Lomb, N.R., Least squares frequency analysis of unequally spaced data, *Astrophys. Space Sci.*, **39**, 447-462, 1976.

Nozawa, S., and A. Brekke, Studies of the auroral E region neutral wind through a solar cycle: Quiet days, *J. Geophys. Res.*, **104**, 45 -66, 1999a.

Nozawa, S., and A. Brekke, Seasonal variation of the auroral E region neutral wind for different solar activities, *J. Atmos. Sol. Terr. Phys.*, **61**, 585 – 605, 1999b.

Pancheva, D., N. Mitchell, H. Middleton, and H. Muller , Variability of the semidiurnal tide due to fluctuations in solar activity and total ozone, *J. Atmos. Solar Terr. Phys*., **65**, 1–19, 2003.

Scargle, J. D, Studies in astronomical time series analysis. II. Statistical aspects of spectral analysis of unevenly spaced data. *Astrophys. J*. **263**, 835, 1982

Night sky condition over Syowa Station deduced from all-sky images by a color digital camera

Satoshi Ishii[1], Hidehiko Suzuki[1], Akira Kadokura[2, 3, 4] and Mitsumu K. Ejiri[3, 4]

[1]*Meiji university*

[2]*Research Organization of Information and Systems, Joint Support-Center for Data Science Research, Polar Environment Data Science Center (ROIS-DS/PEDSC)*

[3]*National Institute of Polar Research (NIPR)*

[4]*Dep. of Polar Science, Sch. of Multidisciplinary Sciences, Graduate University for Advanced Studies, SOKENDAI*

Detailed record of night sky condition (clear, cloudy, partially cloudy, etc.) is essential information to judge the quality of data by ground-based optical instruments. It is important to know a spatial and temporal distribution of lower clouds during observation time for precise analysis of data from instruments with narrow field of view. The method to judge the night sky conditions by detecting stars in a night sky image was proposed by Dr. M. Kubota in 2004 [1]. The automatic weather judgement systems using similar principle have been developed and implemented in previous works (e.g., Nakamura et al., 2019 [2]). We have improved the method to make it available even under aurora condition and applied the method to all-sky image data taken by color digital cameras (CDC) at Syowa Station. CDC is an imager for aurora morphology which have been operated since 2005 at Syowa Station, Antarctic. We have found that CDC is also useful to deduce record of sky condition with high spatial and temporal resolutions after careful calibrations.

In this presentation, we show the record of night sky condition over Syowa Station for 12 years (from 2008 to 2019) deduced by the star counting method. We discuss and verify the seasonal variation of cloud occurrence over Syowa Station. Finally, we propose a usage of the record in data analysis for optical instruments at Syowa Station.

References

[1] National Institute of Information and Communications Technology, Night time cloud amount measuring method and device therefor, JP3593567B2, 2004.

[2] Nakamura R., Takayuki, T., Yasunori, S. and Katsuya, Y., Cloud monitoring system at Telescope Array site by Visible Fisheye CCD, EPJ Web of Conferences 210, 05016, 2019.

Mesospheric ionization impact of energetic electron precipitation during substorm growth phase

Kiyoka Murase[1], Ryuho Kataoka[1, 2], Takanori Nishiyama[1, 2], Koji Nishimura[10], Taishi Hashimoto[1, 2], Yoshimasa Tanaka[1, 2, 3], Akira Kadokura[1, 2, 3], Yoshihiro Tomikawa[1, 2], Masaki Tsutsumi[1, 2], Yasunobu Ogawa[1, 2], Herbert Akihito Uchida[5], Kaoru Sato[4], Satoshi Kasahara[4], Takefumi Mitani[5], Shoichiro Yokota[6], Tomoaki Hori[7], Kunihiro Keika[4], Takeshi Takashima[5], Yoshiya Kasahara[8], Shoya Matsuda[5], Masafumi Shoji[7], Ayako Matsuoka[9], Iku Shinohara[5], Yoshizumi Miyoshi[7], Tatsuhiko Sato[12], Yusuke Ebihara[10], and Takashi Tanaka[11]

[1] *Department of Polar Science, The Graduate University for Advanced Studies, SOKENDAI, Japan*
[2] *National Institute of Polar Research, Japan*
[3] *Polar Environment Data Science Center, Research Organization of Information and Systems, Japan*
[4] *Department of Earth and Planetary Science, The University of Tokyo, Japan*
[5] *Japan Aerospace Exploration Agency, Institute of Space and Astronautical Science, Japan*
[6] *Graduate School of Science, Osaka University, Japan*
[7] *Institute for Space–Earth Environmental Research, Nagoya University, Japan*
[8] *Graduate School of Natural Science and Technology, Kanazawa University, Japan*
[9] *Data Analysis Center for Geomagnetism and Space Magnetism, Kyoto University, Japan*
[10] *Research Institute for Sustainable Humanosphere, Kyoto University, Japan*
[11] *International Center for Space Weather Science and Education, Kyushu University, Japan*
[12] *Japan Atomic Energy Agency, Japan*

Many studies were conducted for the impact of energetic charged particles on the atmosphere during geomagnetically active times, while those in quiet times have still been poorly understood. We found three energetic electron precipitation (EEP) events during the growth phase of moderate substorms and estimate the mesospheric ionization rate for an EEP event in which the most comprehensive datasets from ground-based and space-born instruments were obtained.

The mesospheric ionization signature reached below 70 km altitude and continued for ~15 minutes until the substorm onset, as observed by the PANSY radar, imaging riometer, and all-sky imager at Syowa Station in the Antarctic region. We also used energetic electron flux data observed by the Arase satellite and POES 15 satellite as the input for the air-shower simulation code PHITS to quantitatively estimate the mesospheric ionization rate. The calculated ionization level due to the precipitating electrons was consistent with the observed value of cosmic noise absorption. The possible spatial extent of EEP is estimated to ~8 h MLT in longitude and ~1.5º in latitude from a global magnetohydrodynamic simulation REPPU and the precipitating electron observations by the POES satellite, respectively. Such a significant duration and spatial extent of EEP events suggest a non-negligible contribution of the growth-phase EEP to the mesospheric ionization. Combining the cutting-edge observations and simulations, we shed a new light on the space weather impact of the EEP events during geomagnetically quiet times, which is important for understanding the possible link between the space environment and terrestrial climate.

In this talk, we also show the result of a superposed epoch analysis of the mesospheric echo profiles referring to substorm onset as the zero epoch to quantify how the ionization statistically behaves during the different phases of substorm, and to examine how it depends on the amplitude of substorms, seasons, sunlit conditions etc.

Modeling of SEP-induced auroral emission: Global diffuse aurora on Mars and polar-glow aurora on Earth

Yuki Nakamura[1,2], Naoki Terada[1], Francois Leblanc[2], Ali Rahmati[3], Ryuho Kataoka[4,5], Kiyoka Murase[4,5], Hiromu Nakagawa[1], Shotaro Sakai[1,6], and Sayano Hiruba[1]

[1]*Graduate School of Science, Tohoku University, Sendai, Japan*

[2]*LATMOS/CNRS, Sorbonne Université, Paris, France*

[3]*Space Sciences Laboratory, University of California, Berkeley, CA, USA*

[4]*National Institute of Polar Research, Tokyo, Japan*

[5]*The Graduate University for Advanced Studies, SOKENDAI, Kanagawa, Japan*

[6]*Planetary Plasma and Atmospheric Research Center, Graduate School of Science, Tohoku University, Sendai, Japan*

Solar energetic particles (SEPs) are high-energy particles that consist mainly of electrons and protons with energies from a few tens of keV to GeV ejected from the Sun associated with solar flares and coronal mass ejections. SEPs that precipitate into planetary atmospheres ionize and excite atmospheric molecules, which leads to the auroral emission during SEP events. Such SEP-induced auroral emission have been identified as global diffuse aurora on Mars [Schneider et al., 2015] and polar-glow aurora on Earth [Sandford, 1961]. Space environment of Mars and that of Earth's polar cap region are similar in terms of interaction of SEPs with the atmosphere; SEPs can easily precipitate into the Martian atmosphere everywhere owing to lack of intrinsic magnetic field, and SEPs are guided to the Earth's atmosphere at polar cap region along open magnetic field lines. SEP-induced auroral emission on the two terrestrial planets is still poorly understood; global diffuse aurora on Mars have recently discovered, but it is unknown whether the source is energetic electrons or protons [Schneider et al., 2018], and polar-glow aurora on Earth have not been reported for the past 60 years. Understanding SEP-induced auroral emission is important in evaluating penetration of SEPs into the atmosphere, which in turn lead to the assessment of radiation dose rate on human body, and to the understanding of the effects on chemical changes such as ozone depletion in the middle atmosphere at Earth during SEP events [Jackman et al., 2005] and production of HCN in the early Earth and Mars, which is important in prebiotic synthesis of amino acid [Airapetian et al., 2016; Lingam et al., 2018]. We have developed a Monte Carlo model, Particle TRansport In Planetary atmospheres (PTRIP) to evaluate auroral emission profiles during SEP events on Mars and on Earth. In this talk, we will present the estimation of the emission rates of N_2^+ first negative band in the Antarctic region, estimation of the origin of the global diffuse aurora on Mars by using PTRIP and electron and proton fluxes observed by the Mars Atmosphere and Volatile EvolutioN (MAVEN) spacecraft, and some implications on changes in atmospheric constituents at Mars.

References

Schneider, N. M., Deighan, J. I., Jain, S. K., Stiepen, A., Stewart, A. I. F., Larson, D. et al. (2015). Discovery of diffuse aurora on Mars, *Science*, 350, 6261, doi:10.1126/science.aad0313.

Sandford, B. (1961). Enhancement of Night-Sky Molecular Nitrogen Emission in Polar Cap Absorption Events, *Nature*, 190, 245-246, doi:10.1038/190245a0.

Schneider, N. M., Jain, S. K., Deighan, J., Nasr, C. R., Brain, D. A., Larson, D., et al. (2018). Global aurora on Mars during the September 2017 space weather event, *Geophys. Res. Lett*., 45, 7391-7398, doi:10.1029/2018GL077772.

Jackman, C. H., DeLand, M. T., Labow, G. J., Fleming, E. L., Weisenstein, D. K., Ko, M. K. W., Sinnhuber, M., and Russell, J. M. (2005), Neutral atmospheric influences of the solar proton events in October–November 2003, *J. Geophys. Res*., 110, A09S27, doi:10.1029/2004JA010888.

Airapetian, V., Glocer, A., Gronoff, G. et al. (2016). Prebiotic chemistry and atmospheric warming of early Earth by an active young Sun, *Nature Geosci*., 9, 452-455, doi:10.1038/ngeo2719.

Lingam M, Dong C, Fang X, et al. (2018). The propitious role of solar energetic particles in the origin of life, *ApJ*, 853:10, doi:10.3847/1538-4357/aa9fef.

AuroraX project for space weather and space climate research in Antarctica

Ryuho Kataoka[1], Takanori Nishiyama[1], Akira Sessai Yukimatu[1], Yoshimasa Tanaka[1], Yasunobu Ogawa[1], Akira Kadokura[1], Keisuke Hosokawa[2], Yusuke Ebihara[3], Takeshi Sakanoi[4], Masakazu Watanabe[5], Shigeru Fujita[6], and Takashi Tanaka[5], Kazuoki Munakata[7], Chihiro Kato[7], and Akira Mizuno[8]

[1]*NIPR*

[2]*UEC*

[3]*RISH, Kyoto University*

[4]*PPARC, Tohoku University*

[5]*Kyushu University*

[6]*ISM*

[7]*Shinshu University*

[8]*Nagoya University*

New 6-year Antarctic research project led by JARE and NIPR, called AuroraX project, will start from April 2022. As the most important observation settings for understanding and predicting how the global environment is an open system in space, we will develop a new aurora imaging network in the Antarctic polar cap region via the international collaboration. In addition, the cosmic ray observation at Syowa Station will be fully systemized in order to enable precise measurement of cosmic rays by integrating the global muon detector network and neutron monitors. Further, as a new approach, space-version "reanalysis data" approach is executed in close cooperation with advanced simulations and data science as well as existing observations. While elucidating the physical mechanism of space weather phenomena, the AuroraX project will contribute to solve longer-term and interdisciplinary problems of space climate. In this talk we will present the current situation and future plan in 6 years.

Formation of Polar Cap Plasma Hole

Takahiro Obara[1]
[1]*PPARC, Tohoku University*

In the night side polar cap region, the low density of the ionospheric plasma, called the polar cap plasma hole, was first studied in 1978 (Brinton et al., 1978). They identified the polar hole based on the AE-C satellite data. The polar hole locates poleward of the nightside auroral oval. Minimum O^+ density was as low as $2x10^2$ cm^{-3}. The formation of the polar hole is more often connected to the prolonged recombination in darkness. During the magnetically quiet condition, the polar hole forms as a result of slow anti-sunward convection across the dark polar cap. Crowley et al., 1993 identified a development of polar hole by using a sequential DMSP obsevation over the polar cap region together with sequence of Qaanaaq ionograms. Benson and Grebowsky (2001) identified polar hole just poleward of the nightside oval by using ISIS topside sounder data. They found peak density hight was terrible low; less than 200km, in the polar hole region. Recently, EISCAT Svalbard Radar detected polar hole (Jenner et al., 2020). They have used Super DARN radar data to obtain electric potential patterns and GNSS satellite data to confirm the existence of electron density irregularities around the polar hole region. Results demonstrates that the convection patterns were relatively stable during the interval and little phase scintillation was observed with EISCAT Svalbard Radar.

Vertical sounder experiment, which was carried out by Ohzora (EXOS-C) satellite in 1985, revealed that the polar hole structure appeared in the night side polar cap, extending down to the peak height (~200km) of the ionosphere, and the polar hole was formed in the dead calm period of geomagnetic activity (Obara and Oya, 1989). They compared polar holes observed in the southern hemisphere in September, 1985 and in July, 1986, and found that polar hole regions spread in the winter season. In cases of noon-night passes, plasma density monotonically decreased from the noon side to the night side, forming deep plasma hole just poleward of the night side auroral oval. Based on these studies, it was considered that a formation of the polar hole is more often connected to the prolonged recombination in darkness. During the magnetically quiet condition, the polar hole forms as a result of slow anti-sunward convection across the dark polar cap. The plasma reduces due to the effect of attachment. When the ionized constituent is not supplied sufficiently, a deep hole is formed in the night side polar cap ionosphere (Obara and Oya, 1989).

The present work is a follow up study of Obara and Oya et al. (1985), and the purpose of this study is to obtain loss time constant of O^+ ions and electrons in the dark polar cap ionosphere. In the case of Ohzora (EXOS-C) noon-night pass, plasma density monotonically decreased from the noon side to the night side, forming deep plasma hole just poleward of the night side auroral oval. Example of the plasma hole has been given in Figure 1, where plasma density distribution is given with equi-density contours as a function of height, geomagnetic latitude (Mlat), and geomagnetic local time (MLT). The density unit is log number of electrons/cm^{-3} in Figure 1. The trajectory of Ohzora (EXOS-C) satellite is given by allow. In this case, the satellite traversed polar cap region in the post mid night sector: i.e. from Mlat -71.8, MLT 1.42h to Mlat -84.3, MLT 4.48h. In this pass, a polar hole was clearly identified at regions marked as (b) and (c). A very steep density gradient at (a) corresponds to the night side auroral oval. It is noticed that peak height of the ionosphere was very low; i.e. less than 200km, which seems to be consistent with previous ISIS topside sounder observations (Benson and Grebowsky, 2001). The lowest density detected by Ohzora (EXOS-C) satellite was seen at (b) and it was less than $1x10^3$ cm^{-3}.

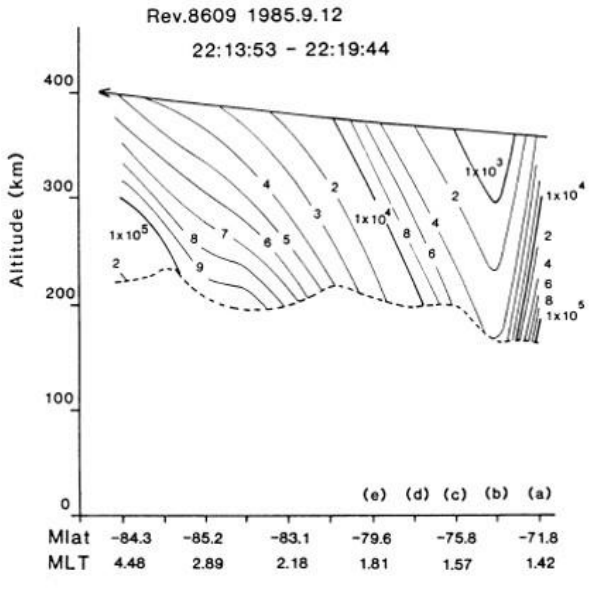

Figure 1. Polar hole observation by Ohzora (EXOS-C) satellite.

Figure 2 demonstrates density profile along the satellite path at 240km, 260 km, 280 km, 300 km and 360 km (left) and orbit of the satellite (right). The satellite traversed polar cap region in the post-midnight sector. We have plotted electron densities at four points (b) to (e), as shown in Figure 1. Electron density reached down to 10^3 cm^{-3} at -76 deg of the magnetic latitude.

Solar wind velocity for this time interval was ~ 340 km/s, and IMF Bz was ~ 0.9 nT, which means that the magnetic condition was low. In such situation, polar cap convection seems to be quite. Assuming that polar cap convection was stable, a density gradients expresses a temporal changes; i.e. $N = N_o \exp(-t / \tau)$. Actually, the distance between (c) and (d) is 400km, it takes 4,000 sec if we assume convection velocity is ~0.1 km/s. The distance between (b) and (c) is same, so it takes another 4,000 sec.

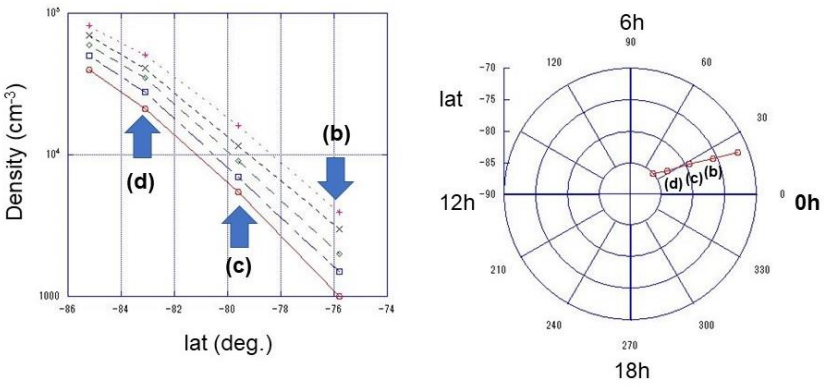

Figure 2. Electron density profile (left) and satellite orbit (right).

Since the electron density is almost same with that of O^+ in the nigh side polar cap, a decrease of the electron density was expressed by the dissociative recombination: i.e. $NO^+ + e \rightarrow N + O$, and $O_2^+ + e \rightarrow O + O$. In this situation, electron loss rate was obtained by $L_e=\beta_1 n(O^+) +\beta_2 n(O^+) = \beta n(O^+)$, where $\beta = \beta_1 + \beta_2$. According to the observation, the electron density will be 1/6 at point (c) and 1/36 at point (b) with respect to point (d), the electron loss time constant was evaluated as ~ 2,000 sec in the night side polar cap region.

In summary, vertical sounder experiment revealed that plasma density monotonically decreased from noon side to night side, forming deep polar hole just poleward of the night side auroral oval and that the plasma hole structure extended down to the peak height (~200km) of the ionosphere. By using an individual noon-midnight pass, we have evaluated loss time constant of electrons. Results demonstrated that loss time constant t is at around 2,000 sec, assuming the weakened convection speed (~0.1km/sec) across the polar cap.

[References]

Benson, R. F., & Grebowsky, J. M., Extremely low ionospheric peak altitudes in the polar hole region. *Radio Science*, 36(2), 277–285, https://doi.org/10.1029/1999RS002401, 2001

Bjoland, L. M., Y. Ogawa, U. Lovhaug, D. Lorentzen, S. M. Hatch, K. Oksavik, Electron density depletion region observed in the polar cap ionosphere, *Journal of Geophysical Research: Space Physics,* doi:10.1029/2020JA028432, 2020.

Brinton, H. C., Grebowsky, J. M., & Brace, L. H. ,The high-latitude winter F region at 300 km: Thermal plasma observations from AE-C, *Journal of Geophysical Research, 83(A10)*, 4767–4776, https://doi.org/10.1029/JA083iA10p04767, 1978

Crowley, G., Carlson, H. C., Basu, S., Denig, W. F., Buchau, J., & Reinisch, B. W., The dynamic ionospheric polar hole, *Radio Science*, 28(3), 401–413, 1993

Jenner, L. A., Wood, A. G., Dorrian, G. D., Oksavik, K., Yeoman, T. K., Fogg, A. R., et al., Plasma density gradients at the edge of polar ionospheric holes: the absence of phase scintillation. *Annales Geophysicae*, 38(2), 575–590, https://doi.org/10.5194/angeo-38-575-2020, 2020

Obara, T. and H.Oya. , Plasma Conditions in the Polar Ionosphere Observed in SPW Experiments of PPS System on Board the Ohzora (EXOS-C) Satellite, *J. Geomagn. Geoelectr.*, 37,285, 1985

Obara, T. and H. Oya., Observations of polar cusp and polar cap ionospheric irregularities and formation of ionospheric holes using topside sounder onboard EXOS-C (Ohzora) satellite, *J. Geomagn. Geoelectr.*, 41, 1025–1042, https://doi.org/10.5636/Jgg.41.1025, 1989

SENSU SuperDARN JARE phase X and future direction

Akira S. Yukimatu[1,2], Nozomu Nishitani[3], Tsutomu Nagatsuma[4], Tomoaki Hori[3], Keisuke Hosokawa[5], Masakazu Watanabe[6], Hideaki Kawano[6], Yusuke Ebihara[7], Hideo Maeno[4], Ryuho Kataoka[1,2], Yoshimasa Tanaka[1,2,8], Koji Nishimura[7], Natsuo Sato[1] and Yuka Kadowaki[8]

[1]*National Institute of Polar Research (ROIS/NIPR), Tokyo, Japan*
[2]*Dep. of Polar Science, Sch. of Multidisciplinary Sciences, Graduate University for Advanced Studies, SOKENDAI, Japan*
[4]*Institute for Space-Earth Environmental Research (ISEE), Nagoya University, Japan*
[3]*National Institute of Information and Communications Technology (NICT), Japan*
[5]*The University of Electro-Communications (UEC), Japan*
[6]*International Center for Space Weather Science and Education (ICSWSE), Kyushu University, Japan*
[7]*Research Institute for Sustainable Humanosphere, Kyoto University, Japan*
[8]*Polar Environment Data Science Center (PEDSC), Res. Org. of Information and Systems (ROIS), Tokyo, Japan*

SuperDARN (Super Dual Auroral Radar Network) is an international high-frequency coherent radar network established in 1995 to observe ionosphere and upper atmosphere on a global scale. More than 35 radars are currently operated by more than 15 research institutes in about 10 countries, distributed from middle to polar latitudes in both hemispheres. One of the original scientific goals of the network was to obtain real-time global plasma convection and electric field potential maps, which had never been done before, to contribute primarily to space weather research. It can also address many aspects of scientific questions on the global upper atmosphere including neutral atmosphere and its coupling with ionised atmosphere, influence of geospace on lower atmosphere and possible global climate change, plasma physics, and practical applied physics including space weather nowcast/forecast. NIPR has joined the SuperDARN project since its establishment in 1995 and has been running 2 SENSU (Syowa South & East HF Radars of NIPR for SuperDARN) radars, that is, Syowa South and Syowa East radars in Antarctic Syowa station (69.00 S, 39.58 E) in the polar auroral zone. Both radars have substantially contributed to the international project and scientific research, e.g., studies on auroral phenomena and storms/substorms, geomagnetic pulsations, precise neutral wind around mesopause region using meteor echoes, studies on polar mesospheric summer echoes (PMSEs), magnetosphere-ionosphere-neutral atmosphere vertical coupling, studies on influence of low solar activity or grand minimum on geospace space weather.

Long-term plan-making of next Phase X 6-year JARE project (JARE 64-69, 2022-2028) starting effectively next year has been discussed and mostly finalised last two years especially on Prioritized Research Projects (PRP) and long-term monitoring observation. We have devoted much time to new space weather and upper atmosphere research with SuperDARN, and our international community has published several tens of cutting-edge scientific papers every year since 1990s. On the other hand, "Space weather maps" - global ionospheric convection and electrical potential maps - with high temporal resolution (of about 1 to 2 mins typically) obtained from the international network data (in quasi-real time) have been widely utilised for a variety of space weather research and prediction works and the number of papers citing SuperDARN has also almost monotonically increased and have exceeded more than 1000 papers per year recently (meaning h-index of SuperDARN as a community is more than 40). The number of research groups, HF radars joining SuperDARN and its total fields-of-view covering the upper atmosphere has also grown. Hence this basic data obtained by SuperDARN has been increasingly important in the modern upper atmosphere research, which means it is of great importance to keep this observation going on a long term basis and to provide the basic valuable data to the wide community.We have reached a conclusion that we should maintain and even acceralate Syowa SENSU SuperDARN project as an essential long-term scientific monitoring observation from the upcoming phase X JARE project for long-term stable contribution to a wider coverage of research and applications, which can also contribute to the PRP on space weather and space climate research proposed by Kataoka et al. (See Kataoka's presentation on Aurora X project in this symposium). Their proposal tries to reveal the impact of high energy particles on the Earth's atmosphere with cosmic ray observations and new spectral riometers etc, and also to understand the geospace environment quantitatively under a lower solar activity where polar cap region observation, such as optical imager network in Antarctica, is essential and important for understanding and predicting geospace under recently started lower solar activity condition after about a half-century long high solar activity period in collaboration with theoretical and simulation studies. In the proposal, SuperDARN is characterised as one of the important tools to provide the global ionospheric condition to contribute to the research.

We will discuss tangible and realistic scientific strategy of SENSU/SuperDARN research including the PRP on space weather/climate and required/desired technical improvement for stabler, near-maintenance-free and more flexible opration including upgrading antennae and transmitters and imaging capability during JARE phase X period.

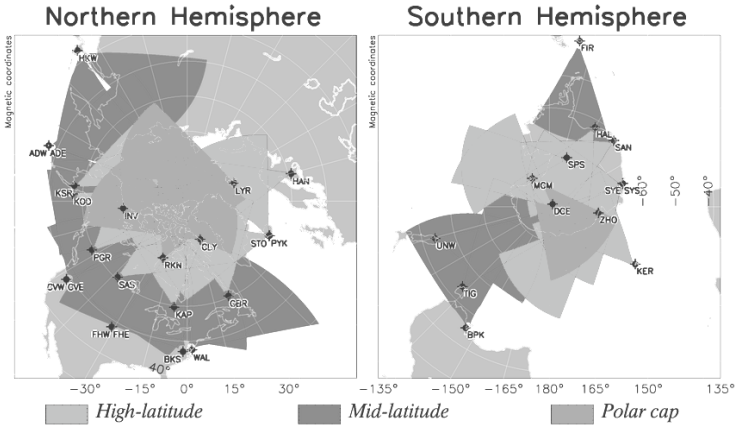

Fields of view of SuperDARN radars in both hemispheres as of 2021 (Courtesy of Virginia Tech SuperDARN group at vt.superdarn.org).

Analysis of the Summer Solstice Storm 2015 based on the “reanalysis data” of the space weather

S. Fujita[1,2], T. Nishiyama[3], A. Kadokura[1,3], and Y. Tanaka[1,3]
[1]*Joint Support-Center for Data Science Research, ROIS*
[2]*The Institute of Statistical Mathematics, ROIS*
[3]*National Institute of Polar Research, ROIS*

The Summer Solstice Storm 2015 has the SC onset at 18h33m on June 22. MMS located in the pre-midnight near-Earth magnetosphere (x ~ -5.7Re, y ~ -7.5Re, z ~ 1.5Re) observed sudden earthward flow at about 5 minutes after the SC onset. The aurora activity was enhanced at this time. Besides, Pc5 pulsation activity was seen in the afternoon at Syowa Station, Antarctica, and its conjugate points intermittently in the recovery phase (13h30m-20h00m on June 23) of this storm. PsA activity was also detected in the Syowa Station.

To understand magnetospheric dynamics in this storm, we need 3-dimensional global information on the plasma disturbances. The present study employs the output of the improved REPPU code. This code is an improved one from the original REPPU code, that is to say, the code incorporates the effect of the rotation of the rotational axis of the Earth, the inclination of the magnetic axis from the rotational axis, as well as the three components of the IMF of OMNI data. Furthermore, this simulation results can be called the “reanalysis data” of the space weather because NICT operates the real-time simulation of the space weather based on a similar code. We use the ionospheric conductivity distribution as the same as the previous version of REPPU code because the code is proved to reproduce the ionospheric potential so well.

The “reanalysis data” calculated by the improved REPPU code employs the Level2 OMNI solar wind data on June, 22-23. We focus on the two events in this storm. First, we treat the sudden onset of earthward flow after about 5 minutes to the SC observed by MMS. We should note that the simulation does not show the one-to-one correspondence to the in situ magnetospheric observations from satellites. However, the simulation results catch the reconnection in the pre-midnight magnetosphere and enhanced earthward flow along with the plasma sheet to the ionosphere. Second, we discuss the intermittent Pc5 pulsation in the recovery phase of this storm (Jun/23/13h30m-20h00m). The calculated Keogram of the FAC in the ionosphere at the local time of Syowa Station exhibits periodic poleward moving form. This result seems similar to the observed periodic auroral activity at Syowa Station. Furthermore, the “reanalysis data” show cyclic plasma disturbances in the dusk-side magnetopause region. Probably, these disturbances are generated by the Kelvin-Helmholtz instability.

We do not insist that the present “reanalysis data” of the space weather is as perfect as the meteorological reanalysis data. The reliability of the data is not so high. While it is quite difficult to obtain the global magnetospheric processes from only the ground-based and in situ satellite observations. To grasp the global feature of the magnetospheric dynamics, the present data are very useful. We plan to proceed with the calculation and open the results and analysis tools to the public. At the same time, we plan to apply the data assimilation technique to obtain more reliable reanalysis data.

.

Acknowledgment

This research is a part of “infrastructure development for the global reanalysis data of the magnetosphere-ionosphere system” (Member: S. Nakano, S, Fujita, A. Kadokura, Y. Tanaka, R. Kataoka, A. Nakamizo, Y. Kubota, K. Hosokawa, and. S. Saita) supported by "Challenging Exploratory Research Projects for the Future" grant from ROIS (Research Organization of Information and Systems).

Modular Design for the Reproduce Plasma Universe (REPPU) code

Satoko Saita [1], Shigeru Fujita[2] and Takashi Tanaka [3]
[1]*National Institute of Technology, Kitakyushu College*
[2] *Joint Support-Center for Data Science Research, Research Organization of Information and Systems(ROIS-DS)*
[2]*International Center for Space Weather Science and Education (ICSWSE), Kyushu University*

The Reproduce Plasma Universe (REPPU) code was developed to reproduce the coupled solar wind-magnetosphere-ionosphere system. The source code is written in Fortran programming language and have been performed on supercomputers.

A complex model composed of a magnetohydrodynamics (MHD below) model and a magnetosphere-ionosphere interaction model is integrated into this code. Then the REPPU code becomes larger, the more costs for developments and operations we will need. Therefore, we propose to partially rewrite and to modularize the source code so that the development cost and the calculating delay time will be reduced.

In this study, we rewrite some part of the REPPU simulation code including conditional branch instructions and repeat instructions into C. The calculation delay time of the modular code indicates the efficiency improvement calculation of the the simulation model.

References

Tanaka, T. (2015), Substorm auroral dynamics reproduced by the advanced global M-I coupling simulation, In Auroral dynamics and space weather, Geophys. Monogr. Ser., vol. 215, edited by Y. Zhang and L. J. Paxton, p. 177, doi: 10.1002/9781118978719, AGU, Washington D. C.

Correction of atmospheric effect on cosmic ray count rate by machine learning

S. Asano[1], R. Kataoka[2],C. Kato[1], A. Kadokura[2],
and K. Munakata[1]
[1]*Shinshu University*
[2]*National Institute of Polar Research*

Cosmic rays are high energy charged particles generated and traveled from outer space. They interact with the Earth's atmosphere and product secondary particles, such as muons, which are detected on the ground. Muon count rate on the ground affected by changing of barometric pressure and atmospheric temperature. These effects on muon count rate are called pressure effect, and temperature effect, respectively.

We have to correct these effects for accurate measurement and analysis of cosmic rays. Pressure effect is able to be corrected straightforwardly, because it uses the pressure observed at the detector site. For the temperature effect, however, it is harder to be corrected, because of the integral effect from top of atmosphere to the ground. Recently, temperature correction method was proposed by Mendonça, et.al. (2019) for Global Muon Detector Network (GMDN) using atmospheric temperatures at various altitudes obtained from Global Data Assimilation System (GDAS). We propose another method to correct the atmospheric effect by a machine learning technique, called Echo State Network (ESN). The training data sets are temperature time series at various altitudes (input) and muon count rate (output).

We applied the trained ESN model to reproduced Syowa muon data by inputting the temperature data. Figure 1 shows the preliminary result of atmospheric effect correction (subtraction of the model data from raw data) by our ESN model. In this presentation we will compare the performance of Mendonça method and ESN model.

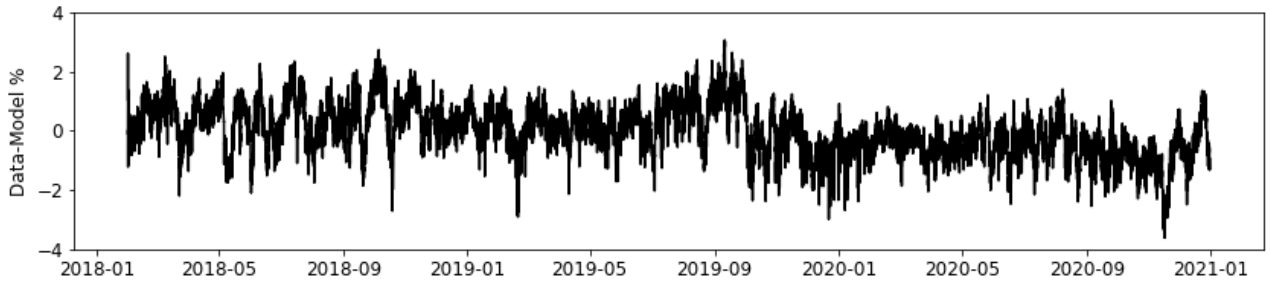

Figure1. Cosmic Ray corrected atmospheric effect by machine learning

References

R.R.S. Mendonça, et.al., Analysis of cosmic rays' atmospheric effects and their relationships to cutoff rigidity and zenith angle using Global Muon Detector Network data, *JGR*, accepted, 2019 (doi: 10.1029/2019JA026651)

Magnetospheric-density estimation from SuperDARN VLOS data to identify magnetospheric regions, by identifying FLR events in ionospheric or ground/sea backscatters

Hideaki Kawano[1], Akira Sessai Yukimatu[2], Nozomu Nishitani[3], Yoshimasa Tanaka[2], Satoko Saita[4], and Tomoaki Hori[3]

[1]*International Center for Space Weather Science and Education, Kyushu University, Japan*

[2]*National Institute of Polar Research, and Department of Polar Science, SOKENDAI, Japan*

[3]*Institute for Space-Earth Environmental Research, Nagoya University, Japan*

[4]*National Institute of Technology, Kitakyushu College, Japan*

Where the frequency of waves coming into the magnetosphere matches the eigenfrequency of a geomagnetic field line, which runs through the ground, the ionosphere, and the magnetosphere, FLR (field-line resonance) can cause the eigen-oscillations of the field line. The FLR-generated eigen-oscillation can be identified from the combination of the maximum in its power and the steepest change in its phase at its eigen-frequency (called the FLR frequency below). From thus identified FLR frequency one can estimate the density along the magnetic field line, because, in a simplified expression, 'heavier' field line oscillates more slowly.

Since the pulsations oscillate the ionospheric plasma, too, there could exist cases in which SuperDARN radars monitor the two-dimensional (2D) distribution of the FLR frequency, from which we can estimate 2D plasma-density distribution on the magnetospheric equatorial plane, including the location of the plasmapause. However, visual identification of the FLR in the SuperDARN VLOS (Velocity along the Line of Sight) data is time-consuming, and the visual identification could miss small-amplitude FLR events and "hidden" FLR events which are superposed by non-FLR perturbations. In addition, there are lots of VLOS data to be analyzed.

Thus, we have been developing a computer code to automatically identify the FLR for any beam of any radars, by using the amplitude-ratio method and the cross-phase methods; these methods cancel out the superposed non-FLR perturbations by dividing the data from a Range Gate (RG) by the data from a nearby RG along the same beam, because the FLR frequency tends to depend on the latitude more strongly than the superposed non-FLR perturbations. Another advantage of applying these methods to the SuperDARN VLOS data is that we can choose any pair of RGs (along the same beam) with different distances, and thus can identify what distance is the best to identify the FLR. This distance reflects the resonance width, which is an important quantity reflecting the diffusion and dissipation of the FLR energy. In the early phase of the code development, we confirmed that the code identified FLR events which we had visually identified in a few beams of a few radars.

The code needs to automatically distinguish whether the identified FLR was in the ionospheric backscattered signal or in the ground/sea backscattered signal; for the latter, the code needs to find the ionospheric reflection point, which is the actual location of the observed FLR. We have implemented these features and tested them for a few radars, and found that the ground/sea events tend to be located at latitudes near the latitudes of simultaneously-observed ionospheric events. We have also calculated, for each event, the corresponding magnetospheric equatorial density; we will show and discuss the density distribution at the meeting.

By using the code we expect to identify much more FLR events than by visual identification; the automatically identified FLR events would include events simultaneously observed at several locations by several radars, increasing the possibility of monitoring the 2D distribution of the plasma density on the magnetospheric equator and identifying magnetospheric regions.

Preparations and objectives for the 4 December 2021 solar eclipse over Antarctica

Mervyn Freeman[1], Michael Hartinger[2], Xueling Shi[3], and James Weygand[4]
[1]*British Antarctic Survey, Cambridge, UK*
[2]*Space Science Institute, USA*
[3]*Virginia Polytechnic Institute and State University, Blacksburg, Virginia, USA*
[4]*Institute of Geophysics and Planetary Physics, University of California, Los Angeles, California, USA*

On 4th December 2021 a total solar eclipse will pass over West Antarctica, and a partial solar eclipse will be experienced over all of Antarctica. An eclipse at such high latitudes is relatively rare and may be expected to affect space weather in both hemispheres, because space weather is concentrated in and couples the two polar regions. In this presentation we will summarise the international array of instruments being coordinated to measure the space weather effects of the eclipse and discuss some of the key scientific objectives. In particular, we will focus on how the reduction in solar illumination affects the ionospheric conductivity and whether this can in turn perturb the geomagnetic field and related magnetosphere-ionosphere current systems.

Optical and radar observations of neutral heating by auroral electrodynamics

Daniel Whiter[1] and David Price[1]
[1]*University of Southampton, UK*

The aurora can have strong electric fields and currents associated with it, which deposit a significant amount of energy in the neutral upper atmosphere through heating. Such heating must be included in global atmospheric models used to study and forecast thermospheric dynamics and chemistry, coupling between the atmospheric layers, climate, and drag on spacecraft and space debris in low Earth orbit. However, the heating rate is poorly quantified, and often spatial structure is not well represented. Heating is typically estimated by measuring the ionospheric electric field using radar, which is then combined with measurements or estimates of the neutral wind velocity and Pedersen conductivity to calculate a Joule heating rate. However, such measurements of the electric field necessarily neglect spatial and temporal variability through their relatively coarse resolution and averaging. The Joule heating rate is proportional to the square of the electric field, and therefore the spatial and temporal averaging lead to a significant underestimate of the Joule heating rate [Codrescu et al., 1995]. As a step towards improving estimates of neutral heating, we observe the thermospheric neutral temperature at high-resolution, bypassing problems associated with coarse electric field measurements.

The University of Southampton operates a high-resolution spectrograph (High-Throughput Imaging Echelle Spectrograph, HiTIES) and multi-spectral narrow field-of-view imager (Auroral Structure and Kinetics, ASK) on Svalbard, in the high Arctic. We have developed a novel technique utilising simultaneous observations from HiTIES, ASK, and the EISCAT Svalbard Radar (ESR) to estimate the neutral temperature altitude profile between approximately 80 km and 200 km altitude at high cadence down to 0.5s [Price et al., 2019]. Applying the technique to observations of an auroral event has revealed very steep horizontal gradients in neutral temperature immediately adjacent to an auroral arc, which we attribute to Joule heating associated with a very strong but localised electric field. In addition, we have identified localised heating inside an arc associated with strong field-aligned currents embedded within auroral curls.

In parallel to the development of the new technique described above, we have installed a combination of optical filters on the ASK cameras which allow imaging of the neutral temperature at E-region altitudes at a spatial resolution of 10s of metres and cadence of 32 Hz; at least an order of magnitude improvement over other similar measurements. Interpretation of such observations is currently ongoing, and preliminary results will be presented.

The EISCAT_3D radar system, which is currently under construction in northern Fenno-Scandinavia, will enable volumetric measurements of ion velocities, and hence electric fields. We plan to combine our optical measurements with measurements from EISCAT_3D to further improve our understanding of the links between auroral electrodynamics and neutral heating, and in particular to quantify the variability and scales involved.

References

Codrescu, M., T. Fuller-Rowell, and J. Foster, On the importance of E-field variability for Joule heating in the high-latitude thermosphere, Geophysical Research Letters, 22(17), 1995.
Price, D. J., D. K. Whiter, J. M. Chadney, and B. S. Lanchester, High-resolution optical observations of neutral heating associated with the electrodynamics of an auroral arc, J. Geophys. Res., 124, 2019.

Effects of CIR- and CME-driven magnetic storm on ion upflows in the low-altitude ionosphere

Masayoshi Takada[1], Kanako Seki[1], Yasunobu Ogawa[2]
[1]*The University of Tokyo*
[2]*National Institute of Polar Research*

Molecular ions ($O_2^+/NO^+/N_2^+$) in the ring current of the terrestrial magnetosphere have been observed during the magnetic storms [e.g., Klecker et al., 1986; Seki et al., 2019]. These ions originate from the low-altitude ionosphere. In the ionosphere, upward ion transports (upflows) supply sources of the ions outflowing to the magnetosphere. Since the molecular ions usually exist in the low-altitude (< 300 km) ionosphere and can be affected by neutral winds, the generation mechanisms and properties of ion upflows to transport molecular ions are different from those of O^+ [e.g., Ogawa et al., 2010; Yamazaki et al., 2017]. In particular, their dependence on solar activities is one of the important properties to understand formation mechanisms of the ion upflows. In a previous study by Ogawa et al. [2019], the characteristics of O^+ ion upflows in the polar ionosphere were investigated during CIR- and CME-driven magnetic storms by using EISCAT radars. They reported that the upflows during CIR- and CME-driven storms have different dependence on magnetic local time: CME-driven storms have about 4 times larger upward ion flux in the nighttime than those under CIR-driven storms and dayside ion upflows under small CIR-driven storms continue a few days longer than those under small CME-driven storms. Their study focused on the ion upflows in the altitude range between 400 and 500 km, where O^+ is the dominant species, and responses of the ion upflows to the different type of magnetic storms in the low-altitude ionosphere, where molecular ions exist, are far from understood. The purpose of this study is thus to understand effects of CIR- and CME-driven magnetic storms on ion upflows in the low-altitude ionosphere based on long-term observations of the EISCAT radars.

We used data from the EISCAT UHF radar at Tromsø and Svalbard radar at Longyearbyen from January 1, 1996 to January 1, 2016, and investigated statistical properties of ion upflows and ionospheric conditions during CIR- and CME-driven magnetic storms. We used 5-minute time resolution data when the radar was looking along the local magnetic field line. The ionospheric parameters such as electron density, ion velocity, and ion and electron temperatures were averaged over 250-350 km altitudes. We screened data to exclude unrealistic values with the following criteria: Absolute value of ion velocity was less than 1500 m/s, ion and electron temperatures were less than 10000 K, and electron density was more than 10^{10} m^{-3} and less than 10^{13} m^{-3}. We also selected reliable data based on the error values of ion and electron temperature: The error value was less than 50% of each temperature. To understand the similarity and difference between low- and high- altitude upflows, we compared data at different altitude ranges using results from the previous study [Ogawa et al., 2019]. The results show that the upward velocity in the nightside at Tromsø increased with increasing altitude in the main phase of both CIR- and CME-driven magnetic storms. On the other hand, the upward flux in the nightside at Longyearbyen was not enhanced at any altitude after CIR-driven storms, whereas it increased from the low-altitude region after CME-driven storms. It was also confirmed that any effect of the magnetic storms that was remarkable at the higher altitudes reported in the previous study [Ogawa et al., 2019] was not seen in the dayside low-altitude ionosphere at Longyearbyen. In the presentation, we will also discuss dependence of the low-altitude upflows on ion/electron temperature and density.

References

[1] B. Klecker et al., Discovery of energetic molecular ions (NO+ and O2+) in the storm time ring current, *Geophys. Res. Lett.*, 13, 632-635, 1986
[2] K. Seki et al., Statistical Properties of Molecular Ions in the Ring Current Observed by the Arase (ERG) Satellite, *Geophys. Res. Lett*., 46, 8643–8651, 2019
[3] Y. Ogawa et al., Solar activity dependence of ion upflow in the polar ionosphere observed with the European Incoherent Scatter (EISCAT) Tromsø UHF radar, *J. Geophys. Res.,* 115, A07310, 2010
[4] Y. Yamazaki et al., Average field-aligned ion velocity over the EISCAT radars, *J. Geophys. Res. Space Physics,* 122, 5630-5642, 2017
[5] Y. Ogawa et al., Characteristics of CME- and CIR-driven ion upflows in the polar ionosphere, *J. Geophys. Res. Space Physics*, 124, 3637–3649, 2019

Antarctic large area network observation of auroral phenomena using unmanned system: Current status of project in 2021

Akira Kadokura[1], Yasunobu Ogawa[1], Yoshimasa Tanaka[1], Hisao Yamagishi[1], Masaki Okada[1], Ryuho Kataoka[1], Herbert Akihito Uchida[1], Yuichi Otsuka[2], Tetsuo Motoba[3], Natsuo Sato[1], Gunnlaugur Bjornsson[4], Jean Rasson[5], Henri Robert[6], Ashwini K. Sinha[7], and Gopi K. Seemala[7]

[1]*National Institute of Polar Research*
[2]*Nagoya University*
[3]*Johns Hopkins University, Applied Physics Laboratory*
[4]*University of Iceland*
[5]*Royal Meteorological Institute of Belgium*
[6]*International Polar Foundation*
[7]*Indian Institute of Geomagnetism*

Space and upper atmospheric sciences group in the National Institute of Polar Research (NIPR) is now planning to construct an observation network for auroral phenomena along the coast of the Dronning Maud Land in the Antarctica including Japanese Syowa Station, and has developed a Unmanned Auroral Observation system (UAO), which is equipped with a 3-axis fluxgate magnetometer, all-sky auroral imager, GNSS/TEC receiver, and a data communication system using the Inmarsat satellite data link with a low power consumption. The first UAO (UAO-1) had been installed at Amundsen Bay area, which is located about 500 km eastward from Syowa Station, in February, 2017 in the summer operation of the 58th Japanese Antarctic Research Expedition (JARE-58). The second UAO (UAO-2) had been installed at Belgium Princess Elisabeth Antarctica (PEA) Station in January, 2020. Electric power of the UAO-1 is supplied by a hybrid natural energy electric generation system which consists of three sets of 192W wind generators and 8 sets of 62W solar panels, while that of the UAO-2 is supplied from the AC power source of the PEA Station which is generated by a power generation system of the station using nine big wind generators and solar panels. For the UAO, observed magnetometer data (1 sec resolution), GNSS BINEX data (30 sec resolution), daily Keogram and sample image data of the auroral imager, and House Keeping data (temperatures and power voltages) (1 min resolution) are transmitted at every 1 hour via the satellite link system to a server in Japan by FTP, and auroral image data of 1 sec resolution are stored in a memory card of the video encoder in the system. Sample interval and pixel resolution of the transmitted auroral image data are 1 hour (5 minutes) and 640x480 (160x120) for the UAO-1 (UAO-2), respectively. UAO-2 has the other USB memory in the system which can store auroral still image of 1 sec resolution with 640x480 pixel resolution and GNSS BINEX data of 1 sec resolution. PEA Station is maintained during summer season, and becomes an unmanned station during winter season, while the electric power to all the instruments at the station is supplied continuously all through the season. In January, 2020, we had also installed an auroral imager system (AIS) at Indian Maitri Station, which consists of four sets of all-sky imager using Watec cameras: 1) Panchromatic (color) ; 2) Panchromatic (black&white); 3) filtered at 560nm (FWHM:10nm); 4) filtered at 632nm (FWHM:10nm), respectively. Maitri is a year-round station. The auroral imager system is run autonomously. We ask expedition members at Maitri to send daily summary files via E-mail to us. During 2020 season, both the UAO-2 at PEA and the AIS at Maitri had been operated successfully, while operation of the UAO-2 was stopped during 2021 season due to some system troubles. In our presentation, we will talk about current status of the project as of late 2021.

Role of the FAC in transmitting substorm disturbances in the M-I coupling system

T. Tanaka[1]

[1]*Emeritus Professor, kyushu-unversity*

We reproduced the substorm by global simulation and analyzed the development of convection, shear, the dynamo, and the field-aligned current (FAC) at the final stage of the growth phase. From these investigations, we show that the substorm is a manifestation of reconfiguration in global flow dynamics. Ionospheric convection can be understood from two aspects. One understanding is as the potential field generated by the FAC, and the other is as the projection of magnetospheric convection. In order for the two to coincide, the FAC must be transmitted together with the motion. As a consequence, resulting convection must be continuous from the magnetosphere to the ionosphere. We see this connection from drawing of shear to recognize that the substorm is the projection process of transient convection. In the growth phase, convective shear that causes the quiet arc and the Harang reversal (HR) occurs on the open/closed (O/C) boundary along the surface of the plasma sheet with a continuous flow structure from the magnetosphere to the ionosphere. The onset starts from more local flow that is induced by the near-earth neutral line (NENL). A narrow shear commences from the NENL in the mid-tail and extends to the ionosphere to replace growth phase shear. Along a closed magnetic field line connected to the NENL, direct penetration flow, squeezing flow, the near-earth dynamo, release of the HR, and the onset FAC occur successively, and consequently cause the ground onset. Such onset mechanism is quite different from the model adopting the current wedge (CW).

References

Tanaka, T., Ebihara, Y., Watanabe, M., Den, M., Fujita, S., Kikuchi, T., et al. (2021a). Formation and release of the Harang reversal relating with the substorm onset process. Journal of Geophysical Research: Space Physics, 126, e2020JA028170. https://doi. org/10.1029/2020JA028170

Tanaka, T., Ebihara, Y., Watanabe, M., Den, M., Fujita, S., Kikuchi, T., et al. (2021b). Development of the substorm as a manifestation of convection transient, Journal of Geophysical Research: Space Physics, 126, https://doi. org/10.1029/2020JA028942

Tanaka, T., Ebihara, Y., Watanabe, M., Den, M., Fujita, S., Kikuchi, T., et al. (2021c). Roles of the M-I coupling and plasma sheet dissipation on the growth-phase thinning and subsequent transition to the onset, Journal of Geophysical Research: Space Physics, submitted.

A possible origin of the "polar cap bifurcation" during northward interplanetary magnetic field periods

Masakazu Watanabe[1], Dongsheng Cai[2], Peikun Xiong[2], Shigeru Fujita[3] and Takashi Tanaka[1]
[1]*Kyushu University*
[2]*University of Tsukuba*
[3]*The Institute of Statistical Mathematics*

During periods of northward interplanetary magnetic field (IMF), in the ionosphere, the flankside plasma sheet expands poleward, with its polewardmost portion detached from its main body. The sun-aligned arc observed by optical measurements may be a manifestation of this plasma sheet fragment. A similar configuration is also reproduced by global magnetohydrodynamic simulations, although the relevance to the real world is still unclear. Figure 1 represents one example in the Northern Hemisphere obtained by the Reproduce Plasma Universe (REPPU) code. We first made a steady state magnetosphere by running the code for 250 min in physical time (t=0–250 min), under a constant northward IMF with a total intensity of B=6 nT and a clock angle of θ=−45° (IMF By<0). We then switched to another constant IMF stepwise with B=13 nT and θ=−70° (the By sign unchanged). Figure 1 represents the northern polar cap 69 min after the IMF switch (t=319 min). A detached region of closed magnetic flux is seen on the dawnside edge of the polar cap. Conversely, a region of open magnetic flux is intruding in the dawnside plasma sheet. A similar detached closed flux is seen on the duskside in the Southern Hemisphere (not shown here). These "islands" of closed flux in the two hemispheres are magnetically conjugate, threaded by the same field lines. We call the configuration in Figure 1 "polar cap bifurcation," although it is unproved whether the polar cap is bifurcated in the topological sense. The polar cap bifurcation indicates the partial breakdown of the 2-null, 2-separator structure that persists almost all the time in the magnetosphere as a global magnetic topology. The polar cap bifurcation started about one hour after the IMF switch and lasted for about 20–30 min (see also Figure 2). The breakdown of the 2-null, 2-separator structure occurs not in the magnetotail but on the dayside when each null point on the dayside broadens to form a null cluster with the same polarity. Figure 2 shows the time variation of the number of nulls on the dayside in each hemisphere. In the presentation, we discuss the topological transition induced by the IMF jolt and the process leading to the polar cap bifurcation.

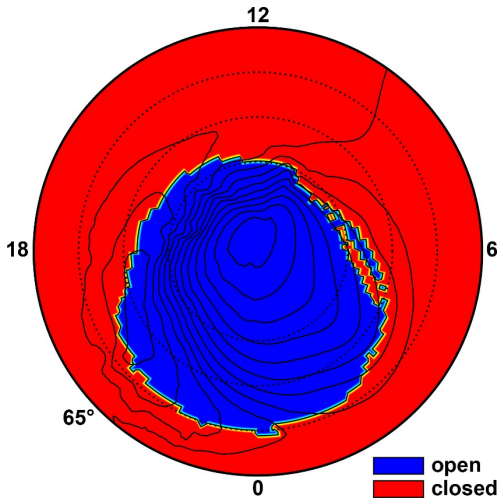

Figure 1. Bifurcated polar cap observed at t=319 min in the Northern Hemisphere (see also Figure 2). The thin black lines represent potential contours every 5kV.

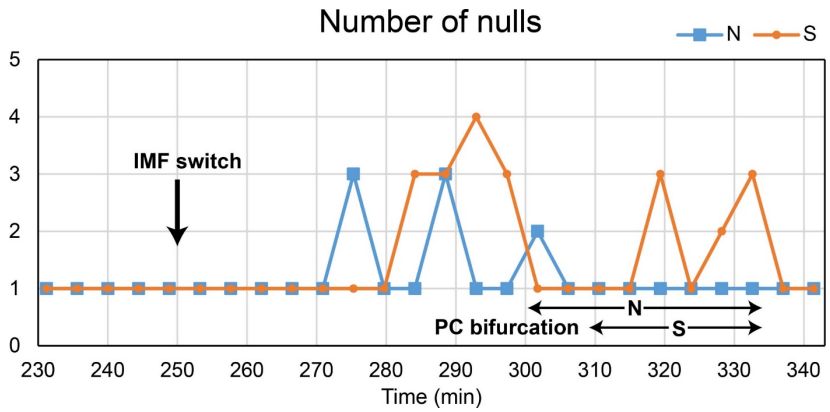

Figure 2. Time variation of the number of nulls in the Northern Hemisphere (N) and in the Southern Hemisphere (S).

The magnetospheric plasma density profile on the Japanese meridian plane: Its dependence on the magnetospheric and sun-related activities

Aoi Onaka[1], Hideaki Kawano[2,3], Teiji Uozumi[2], Shuji Abe[2], and Akimasa Yoshikawa[2,3]

[1]*Department of Earth and Planetary Sciences, Graduate School of Science, Kyushu University, Japan*

[2]*International Center for Space Weather Science and Education, Kyushu University, Japan*

[3]*Department of Earth and Planetary Sciences, Faculty of Science, Kyushu University, Japan*

The purpose of this study is to investigate the spatial distribution of the magnetospheric plasma density and its dependence on the solar and magnetic activity on the Japanese meridian plane.

Where the frequency of fast-mode waves entering the magnetosphere from the solar wind is equal to the natural frequency of the Earth's magnetic field lines, Alfven waves are generated by FLR (Field Line Resonance). The Alfven wave then propagates to the ground and vibrates the H component of the magnetic field. By applying the two-point method (collective name for the amplitude-ratio method and the cross-phase method) to the H-component of the data from two adjacent ground magnetometers, we can obtain the FLR frequency at the midpoint of the two ground magnetometers, and we can estimate the magnetospheric plasma density from the FLR frequency.

While the above method has been used to estimate the spatial distribution of magnetospheric plasma density in the meridian plane of the United States and Europe, the spatial distribution of the magnetospheric plasma density in the meridian plane of Japan has not been estimated because there are few pairs of observation points with a distance that is generally considered suitable for the amplitude-ratio method and the cross-phase method (about 100 km). However, since the FLR is observed on the dayside, if the spatial profile of magnetospheric plasma density on the Japanese meridian is known, we can continuously monitor the magnetospheric plasma density because one of the three meridians in Japan, the U.S., and Europe will always be on the dayside.

In a previous study, Onoue [bachelor thesis 2016] successfully estimated the magnetospheric plasma density using two station pairs for which the distance between the two paired station are much longer than the distance suitable for the two-point method; the two pairs were located on the Japanese meridian plane, and the two pairs' magnetometers belong to MAGDAS which is maintained by Kyushu University.

Itoyama [master thesis 2020] estimated the magnetospheric plasma density in the same period as Onoue [2016] by using 16 pairs of adjacent MAGDAS magnetometers on the Japanese meridian plane. It was found that the FLR could be observed at multiple points simultaneously and that the FLR events were identified frequently enough for continuous monitoring of the density on the Japanese meridian plane. In addition, Itoyama [2020] proved that the estimated plasma density was significantly close to the plasma density model of Gallagher et al. [2000]. However, the length of the observation period of Onoue [2016] and Itoyama [2020] was not long enough so that the number of events was insufficient to investigate the dependence of the magnetospheric plasma density on the solar activity (F10.7) and the magnetic activity (Dst).

In this presentation, we report, with sufficient accuracy, in what manner the number of station pairs detecting the same FLR event, and the estimated magnetospheric plasma density profile, depend on the solar activity (F10.7) and the magnetic activity (Dst).

Identification of Field Line Resonances using Machine Learning Algorithms

Satoko Saita [1], Akiko Fujimoto[2] and Yuki Obana[3]
[1]*National Institute of Technology, Kitakyushu College*
[2]*Kyushu Institute of Technology Research Center for Data Science*
[2] *Department of Engineering Science, Osaka Electro-Communication University*

The geomagnetic field line resonances (FLRs) whose frequencies are affected by the mass density along the geomagnetic field line is helpful for remote sensing of the plasmasphere. In order to analyze a large amount of geomagnetic data and calculate the plasma mass density, we develop a system to recognize and classify the FLRs from geomagnetic pulsations in the ULF (1~1000 mHz) frequency range observed in New Zealand.

In this study, spectrograms and time series data of geomagnetic field were treated as training, validation, and test dataset for constructing a training model using Convolutional Neural Networks (CNN) and Long Short-Term Memory (LSTM). Above-mentioned method is a new approach for the extraction of geomagnetic pulsations. Then we divided the training datasets into two categories. One is time series data. In this case, we assume that we can use a model based on 1D CNN - LSTM, or a combination of these models. The other is the plots of spectrograms of geomagnetic field are treated as input images for 2D CNN. The results obtained from each method are discussed in terms of their effectiveness for analyzing ULF frequency bands. We then proposed a method for acquiring spectrograms and an example of pre-processing of time series data (using Fast Fourier Transform) for a group of training dataset needed in this case.

Plan and progress report on the imaging receiver system at the SuperDARN Hokkaido East radar

Nozomu Nishitani[1], Yoshiyuki Hamaguchi[1] and Tomoaki Hori[1]
[1]*Institute for Space-Earth Environmental Research, Nagoya University*

A plan of implementing an imaging receiver system on the SuperDARN Hokkaido East radar, one of the mid-latitude SuperDARN radars, will be introduced. This system utilizes the USRP SDR unit, which has been used in the remote receiver of the SuperDARN Hokkaido East radar signal in Nagoya (Nishitani et al., 2021). We already manufactured the 4-channel subset prototype system (out of the whole 20-channel system) and successfully tested it on the radar site in July 2020 (Figure 1). We completed the circuit board design for the signal amplifier for the whole 20-channel system (Figure 2).

With the new imaging receiver system, we expect to obtain the data with a temporal and spatial resolution a few times higher than the existing system. We can deal with a wide variety of scientific phenomena, such as (a) ULF waves with a period shorter than 1 minute, which play a significant role in the transport of energetic particles in the inner magnetosphere. (b) Transient fluctuations (responses) excited by external (IMF / solar wind) and internal (substorm expansion) environmental changes in the ionosphere and magnetosphere. (c) Traveling Ionospheric Disturbances triggered by sudden changes on the earth's surface, such as earthquakes and volcanoes. Details of the plan and the progress report of the imaging receiver system will be presented.

Figure 1. Photo of the 4-channel subset imaging receiver system installed at the SuperDARN Hokkaido East radar site.

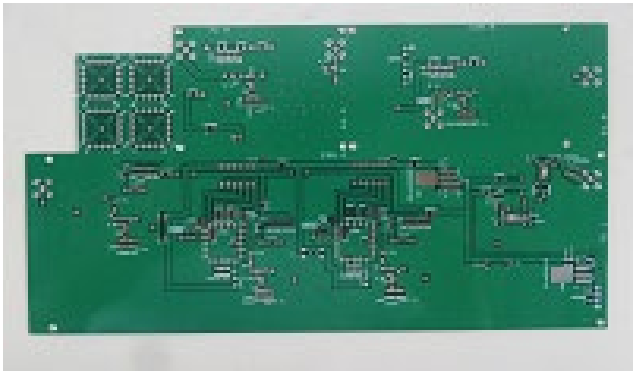

Figure 2. Photo of the circuit board designed for the amplifier of the 20-channel fullset imaging receiver system.

References

Nishitani, N., Y. Hamaguchi, and T. Hori, Development of remote HF wave receiver in the backlobe direction of the SuperDARN Hokkaido East radar: Initial observations, Polar Sci., https://doi.org/10.1016/j.polar.2021.100669, 2021.

Characteristics of wave in the plasmasphere during global-mode wave events: Analysis of data from ground magnetometers at middle and low latitudes

Yuta Yamatani[1], Hideaki Kawano[2,3], Akimasa Yoshikawa[2,3]

[1]*Department of Earth and Planetary Sciences, Graduate School of Science, Kyushu University, Japan*

[2]*International Center for Space Weather Science and Education, Kyushu University, Japan*

[3]*Department of Earth and Planetary Sciences, Faculty of Science, Kyushu University, Japan*

Ultra Low Frequency (ULF) waves (0.2-600s) are frequently observed on the ground at all latitudes. Among them, Pc5 waves have the periodic time of 150-600s, and they are generated by several mechanisms. The global-mode mechanism is one of them; the global modes are fast mode waves trapped between different boundaries of the magnetosphere (the magnetopause, the plasmapause and the equatorial ionosphere). The term global modes include cavity modes and waveguide modes. The cavity mode is the global mode in a closed part of the magnetosphere, so the only energy sink is the ionosphere. On the other hand in the waveguide mode, some portion of the wave energy is leaked into the magnetotail. Global modes have been extensively studied but their existence outside of the plasmasphere was not clearly confirmed until recently. This is because the amplitude is so small that it is easily hidden by other waves with larger amplitudes taking place at the same time. Recently, Hartinger et al. [2012] clearly identified them in data from simultaneous multispacecraft observations in the solar wind, the magnetosheath and the outer magnetosphere, as well as ground magnetometer. Unlike previous observations of global modes outside the plasmasphere, this paper presented the first observations of a global mode when the other wave modes were absent. Hartinger et al. [2013] identified 72 global mode events using electric field, magnetic field, and plasma data from multiple THEMIS spacecraft as well as ground-based observations from 1 February 2008 to 1 April 2010. These papers researched the global modes between the magnetosheath and the plasmapause, but did not make detailed analysis of the waves in the plasmasphere at the event time.

In our research, we will study how such global mode waves are observed at mid and low latitudes on the ground. Thus, we used data from many ground magnetometers around the world, belonging to THEMIS [Russell et al., 2008] or MAGDAS [Yumoto and the MAGDAS group, 2006], and plotted the magnetic field data for the events identified in Hartinger et al. [2013]. In this presentation, we will show the figures, and explain the features of the waves in the plasmasphere when the global modes events occurred.

Atmospheric Electric Field Variations during Auroral Substorm Events

Yasuhiro Minamoto[1], Masashi Kamogawa[1,2], Akira Kadokura[3,4,5], Yoshimasa Tanaka[3,4,5], and Mitsuteru Sato[6]

[1] *Laboratory for Environmental Research at Mount Fuji, Mount Fuji Research Station*

[2] *University of Shizuoka*

[3] *Polar Environment Data Science Center, ROIS-DS*

[4] *National Institute of Polar Research*

[5] *The Graduate University for Advanced Studies, SOKENDAI*

[6] *Graduate School of Science, Hokkaido University*

In order to investigate the global electrical circuit (GEC) modulated by auroral substorm events, the authors studied the variations of atmospheric electric field (AEF) during the substorms using the fair-weather AEF data at Syowa Station, which is located directly under the southern auroral zone.

As the measured AEF in the polar regions is severely affected by blizzards/snowstorms (Minamoto et al., 2021a), the fair-weather periods for the AEF observation should be identified. For this identification, we employed the method proposed by Minamoto et al. (2021b), which used the different AEF data at two different heights under small wind speed (less than 6 m/s). The diurnal variation of the identified AEF values followed the Carnegie curve variation even under the stratiform cloud. To verify the variation of the AEF associated with substorms, we focused on the deviation from the reference diurnal curve of the fair-weather AEF. The reference diurnal curve of the fair-weather AEF was statistically constructed using the data from previous 11 days to post 11 days (i.e., 23 days in total) under the K-index condition of less than 4 regarded as a condition for quiet geomagnetic activity. Representive values and the upper and lower threshold values of the reference diurnal curve were the median, 25th and 75th percentile of the 10-minute bin of the day.

Then, we compared the reference diurnal curve of the AEF and the auroral-related index such as the geomagnetic field at Syowa Station, the Cosmic Noise Absorption (CNA), and the Auroral Electrojet (AE) index. The CNA was used to monitor the precipitation of high-energy auroral particles that caused the ionization in the lower ionosphere (Tanaka et al., 2019).

Figure 1 shows a substorm event on September 2, 2016. K-index was 7 during the period 21UT to 24UT. Observed AEF values were below the 25th percentile of diurnal variation before the increasing of CNA and the onset of the magnetic field disturbance. The AEF was about the 50th percentile of the diurnal variation curve, later than the convergence of the severe magnetic field disturbance and the CNA decreasing. Such a significant decrease in the AEF values during the substorm events was observed in several cases. Since the fluctuations in the AEF due to meteorological conditions such as snowstorms appear as positive anomalies (Minamoto et al., 2021a), these events with negative anomalies of ground-based AEF strongly suggest the existence of ground-based AEF fluctuations associated with the auroral activity.

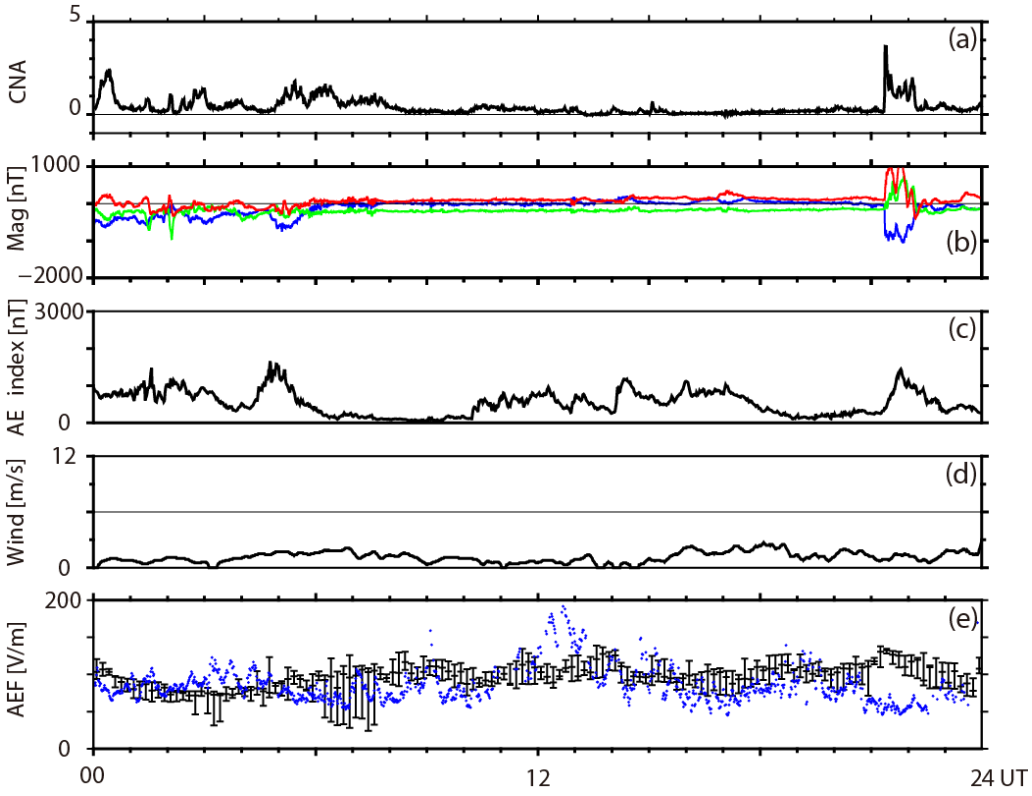

Figure 1. Variations of the CNA, geomagnetic field, AE-index, windspeed and AEF on September 2, 2016.; (a) CNA (b) three componets of geomanetic field, (c) AE-index (d) wind speed (e) AEF. Blue, green and red line in (b) indecates the X, Y, Z component of the geomagnetic field. Bar and whiskers in (e) indicate the reference diurnal variation of the AEF. The 75th, 50th (bar) and 25th percentiles from the top, respectively. Blue dots in (e) indicates the AEF values on the day. Only the fair-weather data were plotted..

References

Minamoto, Y., Kamogawa, M., Kadokura, A., Omiya, S., Hirasawa, N., and, Sato M., Origin of the intense positive and moderate negative atmospheric electric field variations measured during and after Antarctic blizzards. Atmos. Res. 263, 105812., 2021

Minamoto, Y., Kamogawa, M., Kadokura, A , Sato, M. and Omiya, S., A novel methodology of fair-weather identification for ground-based measurement of AEF at the polar region, submitted to J. Geophys. Res.: Atmos., 2021.

Tanaka, Y.-M. , T. Nishiyama, A. Kadokura, M. Ozaki, Y. Miyoshi, K. Shiokawa, S.-I. Oyama, R. Kataoka, M. Tsutsumi, K. Nishimura, K. Sato, Y. Kasahara, A. Kumamoto, F. Tsuchiya, M. Fukizawa, M. Hikishima, S. Matsuda, A. Matsuoka, I. Shinohara, M. Nose, T. Nagatsuma, M. Shinohara, A. Fujimoto, M. Teramoto, R. Nomura, A. Sessai Yukimatu, K. Hosokawa, M. Shoji, and R. Lattecka, Direct comparison between magnetospheric plasma waves and polar mesosphere winter echoes in both hemispheres. J. Geophys. Res.: Space Phys., 124(11), 9626-9639., 2019

Precipitating electron energy of pulsating aurora estimated from all-sky multi-wavelength observations

K. Toyama[1], S. Kurita[2], Y, Miyoshi[1], K. Hosokawa[3], S. Saito[4], Y. Ogawa[5], S. Oyama[1], S. Nozawa[1], T. Kawabata[1] and K. Asamura[6]

[1]Nagoya University, ISEE, [2]Kyoto University, [3]The University of Electro-Communications, [4]NICT, [5]National Institute of Polar Research, [6]Institute of Space and Astronautical Science

Pulsating aurora (PsA) is characterized by quasi-periodic intensity modulations with a period of a few to tens of seconds which is known as the main modulation. Electrostatic Cyclotron Harmonic waves and whistler-mode waves are known to cause the pitch angle scattering of energetic electrons in the magnetosphere. In particular, whistler-mode chorus waves play a crucial role in the pitch angle scattering of electrons. The lower-band chorus causes precipitation of electrons whose energy is greater than several keV [Miyoshi et al., 2015, Kasahara et al., 2018]. It has been shown that the energy of precipitating electrons can be estimated from ground-based optical observations with multi-wavelengths. Ono [1993] observed the emission intensities of PsAs at wavelengths of 427.8 and 844.6 nm using a photometer in Antarctica, and estimated the energy of precipitating electrons by combining the ratio of the emission intensities at the two wavelengths and the model calculation. Since Ono [1993] conducted observations using the instrument with a narrow field-of-view, the energy estimation for 2-D images has not yet been performed. In Tromsoe, Norway, we have operated several highly-sensitive EMCCD cameras, which have simultaneously observed all-sky images of the emission intensity at the two wavelengths (427.8 and 844.6 nm) with a sampling frequency of 10 Hz. In this study, we investigate the spatio-temporal variations of precipitating electron energy using these EMCCD camera data. We estimated the precipitating electron energy of PsA by comparing the emission intensity ratio of the two emission lines using the all-sky image and the emission intensity calculation obtained by the GLobal airglOW (GLOW) model [Solomon, 2017]. The analysis showed that the spatial distribution of precipitating electron energies is not uniform, and a few keV differences are found inside the patch. Besides the optical measurements, we conduct the numerical simulation to derive the ratio of the optical emissions at the two wavelengths, and we estimate the precipitating electron energy. Since the energy spectrum of PsA electrons observed by satellite is not the simple Maxwell distribution, it is expected that the precipitating electron energy derived from the optical measurements is not simple average energy of the precipitating electrons. Our code coupling simulation that combines the test particle simulation GEMSIS-RBW [Saito et al., 2012] that is a wave-particle interactions with the GLOW model, and we find that the energy derived from this method corresponds to the energy at which the maximum energy flux is observed.

References

Kasahara, S., Miyoshi, Y., Yokota, S., Mitani, T., Kasahara, Y., Matsuda, S., Kumamoto, A., Matsuoka, A., Kazama, Y., Frey, H. U., Angelopoulos, V., Kurita, S., Keika, K., Seki, K., Shinohara, I., Pulsating aurora from electron scattering by chorus waves, Nature, 554(7692), 337–340, 2018.

Miyoshi, Y., Satio, S., Seki, K., Nishiyama, T., Kataoka, R., Asamura, K., Katoh, Y., Sakonoi, T., Hirahara, M., Oyama, S., Kurita, S., Santolik, O., Relation between fine structure of energy spectra for pulsating aurora electrons and frequency spectra of whistler mode chorus waves, Journal of Geophysical Research: Space Physics, 120(9), 7728-7736, 2015.

Ono, T., Derivation of energy parameters of precipitating auroral electrons by using the intensity ratios of auroral emissions, Journal of geomagnetism and geoelectricity, 45(6), 455–472, 1993.

Saito, S., Miyoshi, Y., Seki, K., Relativistic electron microbursts associated with whistler chorus rising tone elements: GEMSIS-RBW simulations, Journal of Geophysical Research: Space Physics, 117(A10), 2012.

Solomon, S. C., Global modeling of thermospheric airglow in the far ultraviolet, Journal of Geophysical Research: Space Physics, 122(7), 7834–7848, 2017.

Auroral tomography analysis considering auroral type

Yoshimasa Tanaka[1,2,3], Yasunobu Ogawa[1,2,3], Mizuki Fukizawa[4], Takeshi Sakanoi[4], Keisuke Hosokawa[5], Takuo Tsuda[5], and Akira Kadokura[1,2,3]

[1] *Polar Environment Data Science Center, Joint Support-Center for Data Science Research, Research Organization of Information and Systems*
[2] *National Institute of Polar Research*
[3] *The Graduate University for Advanced Studies (SOKENDAI)*
[4] *Tohoku University*
[5] *The University of Electro-Communications*

Auroral Computed Tomography (ACT) is an analysis technique for reconstructing the three-dimensional (3D) spatial distribution of the auroral luminosity and the energy distribution of the precipitating electrons from auroral monochromatic images taken by simultaneous multi-point imager network observation. More generalized ACT (G-ACT), which was evolved from the ACT, allows us to reconstruct the 3D aurora not only from the multiple monochromatic images but also from other kinds of data, such as the electron density profile measured with the incoherent scatter radar. These methods can be applied to mainly discrete auroras, whose luminosity is bright enough relative to the background diffuse aurora and whose outline is well-defined. However, with the development of high-sensitivity imagers, there is a growing demand to apply these methods to the pulsating aurora. Since it is difficult to reconstruct the 3D distribution of faint pulsating auroras, these analysis methods are required to be improved.
In this study, we summarize the key points when using the ACT and G-ACT methods for reconstructing the discrete auroras and pulsating auroras. The main points are shown as follows; (1) the reduction of the effect of the diffuse auroras, (2) the estimation of the relative sensitivity between imagers, (3) the determination of the hyper-parameters of the regularization term, and (4) the validation of the reconstruction results using model auroras. We will illustrate these methods with some examples of their application to the model and observational data.

Yearly variations in Be-7 concentrations in the surface air at Iceland and Japan for 17 years from 2003: Solar modulation of cosmogenic nuclide

H. Sakurai[1], Y. Kawamura[1], F. Tokanai[1], E. Inui, M. Takeyama[1], T. Moriya[1]
F. Miyake[2], A. Kadokura[3], N. Sato[3], and B. Gunnlaugur[4]

[1]*Faculty of Science, Yamagata University*
[2]*The Institute for Space-Earth Environmental Research, Nagoya University*
[3]*National Institute of Polar Research*
[4]*Science Institute, Iceland University*

Be-7 concentrations (BEC) in surface air should be correlated to cosmic rays, because Be-7 is produced by interactions between cosmic rays and nitrogen and/or oxygen in the atmosphere, and then it falls down with aerosols. Since cosmic rays which reach the earth are modulated by the solar activities when travelling the heliosphere, the variation in BEC involve some modulation profiles such as 27-day variation and 11-year solar cycle. Daily Be-7 concentrations in surface air have been continuously observed at Yamagata (38° N), Japan since 2000. To investigate the latitude effect of 11-year solar cycle, we set up a daily observation system of Be-7 concentration at Husafell in Iceland located (64° N) and have been continuously observed BEC since September 2003 as well as in Japan. Figure 1 shows the daily variations of the BEC in Iceland with the sunspot number (SSN), respectively. As shown in the SSN, the solar cycle 24 began in 2009 and ended in almost 2020 reaching its maximum in 2014. In the lower panel of the figure, while the daily profile of BEC are intensively fluctuating, the yellow smoothed line due to moving average of 180 points indicates a yearly variation corresponding inversely to the solar activity. Also, the red smoothed line due to moving average of 27 points clearly indicates a seasonal variation relating to the atmospheric air-mass motion. The seasonal variation of BEC in Iceland shows an apparent one peak distribution which has the peak and bottom on April and September, respectively. The ratio of BEC on April to that on September was 1.8 on average for 17 years. On the contrary, the seasonal variation of BEC at Yamagata shows bimodal distribution which has two peaks on April and September.

We describe about the difference of the Be-7 concentrations between in Iceland and at Yamagata focusing on their seasonal variations.

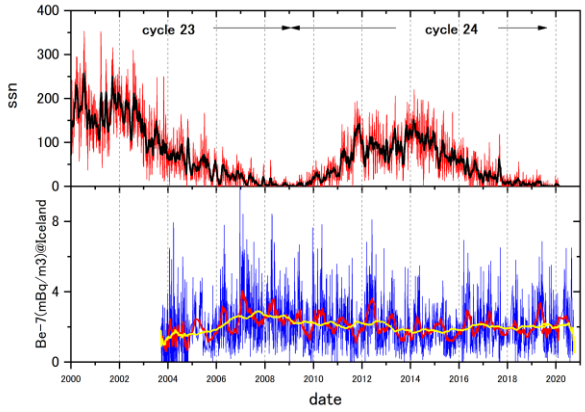

Figure 1. Daily profiles of the Be-7 concentrations and the sunspot numbers